N vacancy, substitutional O, and Al defects in the bandgap of composition-tunable nonstoichiometric AlN powder

Zhang Dian(张 电), Liu Fa-Min(刘发民)†, and Cai Lu-Gang(蔡鲁刚)

Department of Physics, School of Physics and Nuclear Energy Engineering, Beihang University, Beijing 100191, *China*

(Received 12 December 2013; revised manuscript received 19 January 2014; published online 20 April 2014)

AlN powders are prepared by direct nitridation via Al liquid and vapor phases in mixed atmospheres of N_2 and NH_3 with different NH_3/N_2 ratios. The reaction analysis reveals that NH_3 acts as catalyst for N_2 dissociation and the transportations of N, O, and Al in the liquid phase are different from those in the vapor phase. Accordingly, the products are Al-rich and composition-tunable nonstoichiometric AlN in which N, O, and Al content values change with nitridation atmosphere and temperature, leading to the variation of the relevant defect concentration. Therefore, the AlN powders exhibit prominent absorption bands around 5.30, 3.40, and 1.50 eV, which are tentatively assigned to V_N, O_N donors, and Al_N acceptor respectively. Furthermore, a new donor named [V_N–O_N] complex is predicted at 4.40 eV within the 5.90 eV bandgap. It is demonstrated that the optical spectra of nonstoichiometric AlN are preferable to the nominal stoichimometric one for the identification of the defects energy level.

Keywords: III–V semiconductors, defects, optical properties, luminescence

PACS: 78.30.Fs, 68.55.Ln, 78.40.–q, 78.55.–m **DOI:** 10.1088/1674-1056/23/6/067803

1. Introduction

Aluminum nitride (AlN) has aroused the intensive research interest recently due to its wide direct bandgap (6.2 eV) and excellent thermal conductivity, leading to broad applications in the UV-c light (100 nm–280 nm) emitters, detectors,[1–6] UV transparent wafers,[7–11] and power electric devices' substrates.[12–14] Optical absorption (OA), photoluminescence (PL), and cathodoluminescence (CL) could provide an insight into the AlN band structure, defect energy level, and the relevant electronic transitions, which are crucial for the understanding and application of AlN. Although many studies about AlN films,[15–18] bulk single crystals,[19–23] ceramics,[24,25] and powders[26–31] have been reported, there exist contradictions in their results and conclusions about the accurate defect energy levels in the optical spectra and corresponding transitions. Therefore, further research is necessary to identify the detailed band structures and analyze the optical spectra.

In a previous study,[32] we discussed the synthesis process of AlN powders by direct nitridation (DN) in pure N_2 and NH_3 atmospheres respectively and concluded that nonstoichiometric AlN with extensive range of N/Al ratio was produced. Here, we prepare AlN powders in the mixed atmospheres of NH_3 and N_2 with different NH_3/N_2 ratios. By comparison of the results with those prepared in pure N_2 and NH_3, a comprehensive nitridation model is established. Furthermore, the defect energy levels within the bandgap are identified by comparing and tentatively assigning their OA and PL spectra. To the best of our knowledge, there has been no report on discussing the AlN bandgap structure through OA and PL spectra of composition-tunable nonstoichiometric AlN, which would have more prominent optical features related to N, O, and Al defects than the stoichiometric AlN.

2. Experimental section

The raw materials, furnace, configuration, and procedure used in the present experiments were the same as those in a previous study[32] except that NH_3 and N_2 mixture was used as atmosphere in this study. The total mixture flow rate was kept at 5×10^{-6} m^3/s (300 sccm) as in the previous study, while the NH_3/N_2 ratios of the mixture were 1:5, 1:2, and 1:1 respectively. To facilitate the discussion, the atmospheres were marked as A (pure NH_3), B (1:1), C (1:2), D (1:5), and E (pure N_2), in which order the N content value increased and H content decreased. The nitridation temperatures were 1200 °C, 1300 °C, and 1400 °C. For D atmosphere, the nitridation temperature was extended downward to 1100 °C, 1000 °C, and 900 °C to compare the results with those in A and E. Meanwhile, we provided commercial carbonthermal reduction nitridation AlN powders (CRN-AlN) as reference of our direct nitridation AlN powder (DN-AlN).

The product structures were analyzed using an X'Pert Pro XRD system with an operating voltage of 40 kV, a current of 40 mA, Cu Kα wavelength of $\lambda = 0.154059$ nm, and scanning range 2θ from 30° to 80°. The morphologies of the products were studied via an FEG XLs 30 scanning electron microscope (SEM). The chemical composition of the product was obtained from the specimen by energy dispersive x-ray spectrometer in a recommended situation. The optical absorption was measured via Persee TU-1901 double-beam UV-

†Corresponding author. E-mail: fmliu@buaa.edu.cn

© 2014 Chinese Physical Society and IOP Publishing Ltd

spectrophotometer from 190 nm to 900 nm with a 0.1-nm resolution, and the PL measurement was conducted by the He–Cd laser with 325-nm wavelength.

3. Results and discussion

3.1. XRD, morphologies, and compositions analysis

All the products produced in B, C, and D atmosphere at 1200 °C, 1300 °C, and 1400 °C include loose powders in the crucibles and large branches at the brim of the crucibles as shown in the inset of Fig. 1, which has a similar appearance to those of the products in A atmosphere in the previous study. The appearance indicates that the large branches grew via vapor phase mechanism and the loose powders were produced via liquid phase mechanism. The branches and the powders are collected and marked as V and L samples respectively for the following observation. Thus, all samples in this study together with those relevant ones in the previous study[32] are given in Table 1.

Table 1. Nitridation conditions of different samples.

Conditions	A (NH_3)	B (NH_3:N_2=1:1)	C (NH_3:N_2=1:2)	D (NH_3:N_2=1:5)	E (N_2)
1100 °C	1100 A–V	–	–	–	–
	1100 A–L	–	–	–	–
1200 °C	1200 A–V	1200 B–V	1200 C–V	1200 D–V	–
	1200 A–L	1200 B–L	1200 C–L	1200 D–L	–
1300 °C	1300 A–V	1300 B–V	1300 C–V	1300 D–V	–
	1300 A–L	1300 B–L	1300 C–L	1300 D–L	–
1400 °C	1400 A–V	1400 B–V	1400 C–V	1400 D–V	–
	1400 A–L	1400 B–L	1400 C–L	1400 D–L	1400 E–L

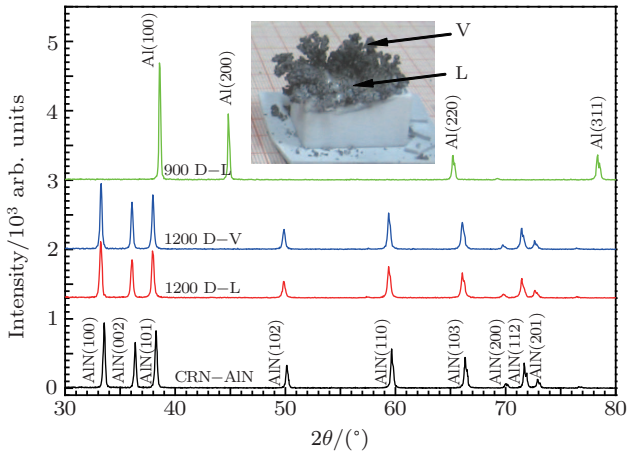


Fig. 1. (color online) XRD patterns of the products with the inset showing large branches of AlN powders (labeled as V) grown at the brim of the crucible and loose powders (labeled as L) produced in the crucible. XRD patterns reveal that sample 900 D–L (L sample prepared in D (NH_3:N_2=1:5) atmosphere at 900 °) is still Al powder, while 1200 D–L and 1200 D–V L and V samples are grown at the brim of and produced in the crucible in D (NH_3:N_2 = 1 : 5 atmosphere at 1200 °C) are converted into pure AlN powders with similar XRD patterns. In contrast to CRN-AlN, the peaks of XRD pattern of DN-AlN (commercial carbon-thermal reduction nitridation AlN) shift toward low 2θ angle slightly, indicating the expansion of lattice constant.

The XRD patterns of the products in D atmosphere as shown in Fig. 1 reveal that the product still reamins pure Al at 900 °C, while full nitridation is accomplished at 1200 °C and there is no apparent difference between L and V samples. Other products in B, C, and D beyond 1200 °C are also pure AlN powders whose XRD patterns are not shown. The XRD patterns of CRN-AlN are shown simultaneously in Fig. 1 for comparison. The only difference between the patterns of DN-AlN and CRN-AlN is in the peak locations, indicating their different plane spacings, such as (100) spacings are 2.6942, 2.6929, and 2.6685 Å for 1200 D–L, 1200 D–V, and CRN-AlN respectively. The lattice expansion of DN-AlN could originate from point defects such as N vacancy, anti-site and/or interstitial Al atom in view of its low N/Al ratio of the composition.

The morphologies of the products and CRN-AlN are shown in Fig. 2, in which figure 2(a) shows that severe passivation occurs at the surface of Al powder in D atmosphere at 900 °C. A dense layer of AlN nanocrystals is coated by Al powder and prevents inner Al from being nitrided, which explains why its XRD pattern belongs to Al. The passivation effect is the same as what happened in A atmosphere in the previous study. The morphology of the product in D atmosphere at 1000 °C (see Fig. 2(b)) reveals that the passivation effect is eliminated because the inner liquid Al burst out of the passivation layer, accelerating the nitridation. When nitridation temperature reaches 1200 °C in B, C, and D atmospheres, massive Al evaporation leads to quick and full nitridation, producing AlN powders in the crucible and large branches at the brim of the crucible as shown in Fig. 2(c). The V sample is composed of nanocrystals with diameters about 20 nm–500 nm while L sample is comprised of micro or submicro grains with diameters about 0.2 μm–2 μm as shown in Figs. 2(d) and 2(e) respectively. The grain size of CRN-AlN is about 0.5 μm–2 μm (see Fig. 2(f)).

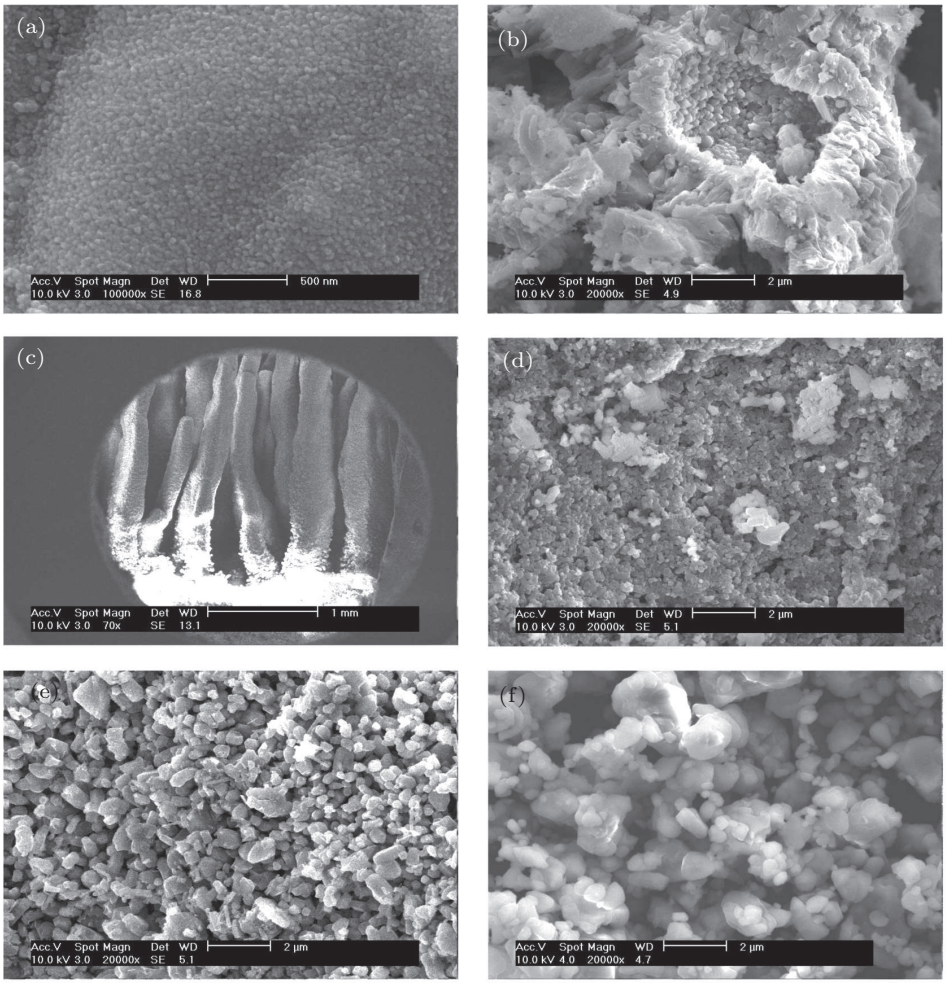


Fig. 2. Morphologies of the AlN powders, where (a) sample 900 D–L shows that the Al powder surface is passivated by nanocrystals layer, (b) sample 1000 D–L reveals that liquid Al burst out of the passivation layer, (c) sample 1200 D–V displays the large branches, (d) enlarged view of the branches exhibits nanocrystals, (e) sample 1200 D–L produced in the crucible indicates submicro grains, and (f) sample CRN-AlN shows large grains.

Composition analyses of the DN-AlN and CRN-AlN indicate that the products are Al-rich and composition-tunable nonstoichiometric AlN with extensive N/Al ratio which varies with temperature and atmosphere as plotted in Fig. 3. The change of composition ratio from stoichiometric value to low N/Al ratio could result from Al particle or cluster incorporation, oxidation, point defects such as N vacancies and interstitial or substitutional Al atoms. Comparatively, N/Al ratio of CRN-AlN is closer to stoichiometry than those of most DN-AlN powers. As a whole, figure 3 reveals that the samples prepared in A and D atmospheres have lower N/Al ratio than those in B and C atmospheres. This implies that more reactive N atoms are released in B and C atmospheres than those in A and D atmospheres. Meanwhile, V sample has relatively high N/Al ratio than L sample. Additionally, EDX reveals that O content value of CRN-AlN was 1.9 at.% and those of DN-AlN samples vary in a range from 2.0 at.% to 6.0 at.%. The composition variation could support the analyses of reaction and defect related optical properties in the following sections.

3.2. Reaction analysis

Since the reaction model of the direct nitridation in pure N_2 and NH_3 has been discussed in a previous study,[32] in this paper we investigate the case of N_2 and NH_3 mixtures.

As illustrated in the previous study, N_2 has a low disassociation rate so that full nitridation can be realized only when the temperature arrives at 1400 °C and no branches grow at the brim of the crucible in E atmosphere. In contrast, NH_3 easily dissociates in the presence of Al powders so that full nitridation is achieved in A atmosphere at temperatures as low as 1100 °C leading to pure AlN powders produced in the crucible and large branches grown at the brim of the crucible. The same things happen when a mixed atmosphere is used even if the NH_3/N_2 ratio is as low as 1/5 in D atmosphere. Furthermore, some research[33,34] reported that full nitridation was obtained even if the NH_3 content value is as low as 5 at.%. Actually, massive AlN branches are collected at the brim of the crucible in D atmosphere at 1200 °C (Fig. 1) while no branch forms in E atmosphere even at 1400 °C. Therefore, it could be pre-

dicted that NH_3 participates in the process of N_2 dissociation in the mixture as expressed by the following equation:

$$N_2 + NH_3 \xrightarrow{\text{surface}} 3N_{\text{suface}} + 3H_{\text{surface}}, \quad (1)$$

namely, NH_3 could act as catalyst in N_2 dissociation so that more reactive N atoms are released in the mixture than in E atmosphere although the former has smaller nominal N content value than the latter. This is just the reason why serious passivation effects take place at 900 °C in D atmosphere as shown in Fig. 2(a). In addition, NH_3 could help eliminate O contamination in Al powders via Eq. (2), resulting in O content variation in the products. Combined with atmosphere variation, nitridation temperature exerts its influence on these reactions.

On the other hand, some essential kinetic factors are different between L and L samples. The species transpositions in liquid and vapor phases comprise both convection and diffusion. Species transposition is easy in the vapor phase and hard in the liquid phase, resulting in relatively rich N in V samples and local shortage of N in L sample respectively. Meanwhile, NH_3 and N_2 dissociate into reactive N species more efficiently in the presence of the interface of the liquid phase, which L samples can provide and V samples cannot. That is why no V samples appear in E atmosphere. Moreover, O contamination in liquid Al is easier to be eliminated at higher temperature because intensive evaporation can trigger convective transportation, which is a rapid transportation channel for H species rather than diffusive transportation. In addition, once an O atom is expelled from liquid Al via the following equation:

$$2NH_3 + Al_2O_3 \rightarrow 2AlN + 3H_2O, \quad (2)$$

it will enter into vapor phase and form an O-rich atmosphere, which could increase O contamination in V samples. Consequently, the concentrations of N and O are different in local circumstances of L and V samples which are produced in different atmospheres and at different temperatures, leading to different point defect concentrations and relevant properties.

According to the analyses in the present study and the previous study, here we put forward a comprehensive reaction model as follows.

(i) NH_3 atmosphere

In pure NH_3 atmosphere, full nitridation is realized beyond 1100 °C producing loose powders in the crucible and large branches at the brim of the crucible. Consequently, the nitridation occurring in NH_3 atmosphere, no matter whether it is in liquid phase or in vapor phase, could be expressed by the following equation:

$$Al + NH_3 \rightarrow AlN + \frac{3}{2}H_2. \quad (3)$$

Nominally, total N content value in A atmosphere (pure NH_3) is lower than those in E atmosphere (pure N_2) and other mixture atmospheres because of the same total flow rate. However, in comparison with N_2, NH_3 has a very high dissociation rate so that the actual concentration of reactive N species in A atmosphere is higher than that in E atmosphere. Meanwhile, the transportation of N species in A atmosphere is very fast because loose accumulation provides a fast transportation channel for nitrogen sources, which does not happen in E atmosphere. Therefore, the product in A atmosphere has relatively high N concentration and N/Al ratio. In addition, the nitrogen source is richer and its transport is faster in the vapor phase than in liquid Al, thus N/Al ratio of the V sample is higher than that of L sample. In another respect, O contamination decreases in the liquid phase because equation (2) occurs in the liquid phase, and it increases in the vapor phase because O becomes rich in the atmosphere. Since A atmosphere has the highest H content value in the experimental conditions, it could produce AlN powder with the lowest O content value.

(ii) NH_3–N_2 mixture atmosphere

In NH_3–N_2 mixture atmospheres of B, C, and D, the nitridation process is similar to that in A atmosphere. However, a catalysis-aided N_2 dissociation process could take place in the mixture atmosphere as expressed by Eq. (1). This leads to varying content values of N, H, O, and N/Al ratio in the final products in different atmospheres. Since nominal N content value increases while the dissociation rate could decease from A to E atmosphere, the reactive N concentration could reach a maximal value in a mixture atmosphere, leading to a maximal N/Al ratio of the product as revealed by Fig. 3. Since the catalysis-aided N_2 dissociation could be complicated and different in the liquid phase from in the vapor phase, here we describe the nitridation in mixture as follows:

$$3Al + N_2 + NH_3 \rightarrow 3AlN + \frac{3}{2}H_2. \quad (4)$$

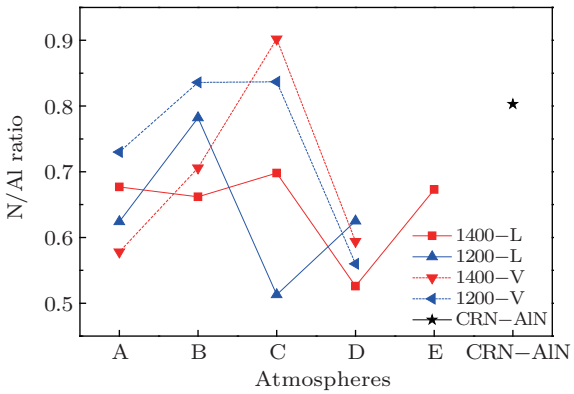


Fig. 3. (color online) N/Al ratios of the composition-tunable nonstoichiometric AlN powders versus atmosphere, revealing that samples prepared in A and D atmospheres have lower N/Al ratio than in B and C atmospheres, V samples have relatively high N/Al ratio compared with L samples, and N/Al ratio of CRN-AlN is closer to stoichiometric value than that of DN-AlN.

(iii) N_2 atmosphere

Full nitridation is realized only at 1400 °C in pure N_2 atmosphere, and the final product is a dense polycrystalline

AlN bulk instead of loose powders. One should note that no AlN branches form at the brim of the crucible, indicating that Al vapor could hardly react with N_2 gas directly even at 1400 °C. Therefore, the nitridation in the liquid phase could be expressed as

$$2Al_l + N_2 \xrightarrow{\text{surface}} 2AlN, \quad (5)$$

while the nitridation could not happen in the vapor phase as indicated by the following equation:

$$2Al_g + N_2 \neq 2AlN, \quad (6)$$

showing the importance of liquid Al surface for N_2 dissociation. Since the dissociation rate of N_2 is low, the local concentration of reactive N in liquid Al is low in E atmosphere, resulting in Al-rich AlN with low N/Al ratio. Besides, O content value in the product cannot decrease due to the absence of H species.

In summary, composition-tunable nonstoichiometic AlN is produced and the content values of N, Al, and O vary with atmosphere and temperature. The composition variation would affect the point defect concentration, which allows us to investigate the point defects and their effects on the optical properties of AlN. Finally, we can investigate defect energy level in the energy band though comparing their optical spectra.

3.3. Optical absorption and PL spectra analysis

Optical absorption spectra of CRN-AlN and DN-AlN produced at 1400 °C are shown in Fig. 4(a), in which the curves are marked with the corresponding sample labels. It shows that all the curves are similar in shape and different in location, meaning that 1400 E–L lie at the upmost location while the curve of CRN-AlN at the bottommost location and others in between. Furthermore, all curves of V samples lie above those of their corresponding L samples in a range from 1.90 eV to 4.20 eV.

The background absorbances of these curves are mainly caused by grain size effect, which shows that smaller particles lead to more light reflection and less light absorption. This is confirmed by 1400 E–L, 1400 E–L1, and 1400 E–L2 samples, among which the latter two are prepared from the former one by grinding for 5 min and 10 min in agate mortar respectively. As shown in Fig. 4(a), the curve indented toward low absorbance value with the increase of grind time but has no change in shape. Therefore, 1400 E–L sample should have the largest grain size in all samples because its absorbance curve is situated above all other curves. This deduction accords with the conclusion in the previous study that low dissociation rate of N_2 caused low N concentration in Al liquid and led to large grain size of AlN powder.[32] Meanwhile, it should be pointed out that multiscattering absorption and structure defects such as stacking default and dislocations, deformation and strain, trace impurity absorption, and phonon replicas of absorption peaks could also influence the absorbance background.[35,36] These factors could explain why V sample always has a smaller particle size and higher absorbance than corresponding L samples. However, all these factors, especially impurity in raw Al powder, are similar to those for DN-AlN samples and could influence the absorbance background rather than the shape of the curve. In other words, the differences between the spectra just arises from those factors in the nitridation process such as atmosphere and temperature. On the other hand, one could realize that all the curves have their minima around 1.90 eV, implying that no defect state was there nominally.

Accordingly, in order to exclude the influences of the background and give prominence to the influences of atmosphere and temperature on the absorption band, the spectra are indented onto transversal axis at their minima around 1.90 eV. In the range from 4.20 eV down to 1.90 eV in Fig. 4(b), the curve for 1400 E–L sample is situated at the upmost location and that for the CRN-AlN at the bottommost location with other curves in between. Meanwhile, all curves of V samples are situated above that of their corresponding L samples in the range. The results are consistent with Fig. 4(a) and the consistency reveals that the indentation of the absorption spectrum is reasonable and reliable.

Commercial CRN-AlN powder is used as reference powders for the DN-AlN powders in order to compare their OA and PL spectra, identify the defect energy level and relevant optical transitions. Generally, the major point defects in unintentionally doped AlN include N vacancy (V_N) and Al vacancy (V_{Al}), substitutional O (O_N), interstitial Al (Al_i) and N (N_i), anti-site Al (Al_N) and N (N_{Al}), and their complexes. Meantime, minor point defects such as interstitial O (O_i), H and impurities related defects could exist. As is well known, CRN-AlN is prepared in a solid phase reaction system at extreme high temperatures above 1700 °C, the nitridation takes place via N atom diffusion. Thus, V_N, O_N, and Al_N rather than V_{Al} and Al_i are its major defects. In addition, C-related defect could appear since carbon reductant incorporates into AlN lattice. For our DN-AlN, L samples are produced in Al liquid phase, and the nitridation takes place mainly via N diffusive transportation which results in lack of local N atoms. Therefore, V_N, O_N, Al_N, and Al_i should be major defects while V_{Al}, N_{Al} and others should be minor defects. O contamination originates from impurities in both Al powder and nitrogen source. Since V samples are formed by the vapor phase, its V_N should be lower than those of L samples, owing to easier transportation and higher concentration of N. Moreover, O_N should be higher in V sample than that in L sample because O expelled from liquid and O impurity in nitrogen source both increase O content value in atmosphere, leading to O incorporation into AlN lattice. Besides, H doping could affect the spectra of the DN-AlN obtained in pure NH_3 and the complex atmospheres.

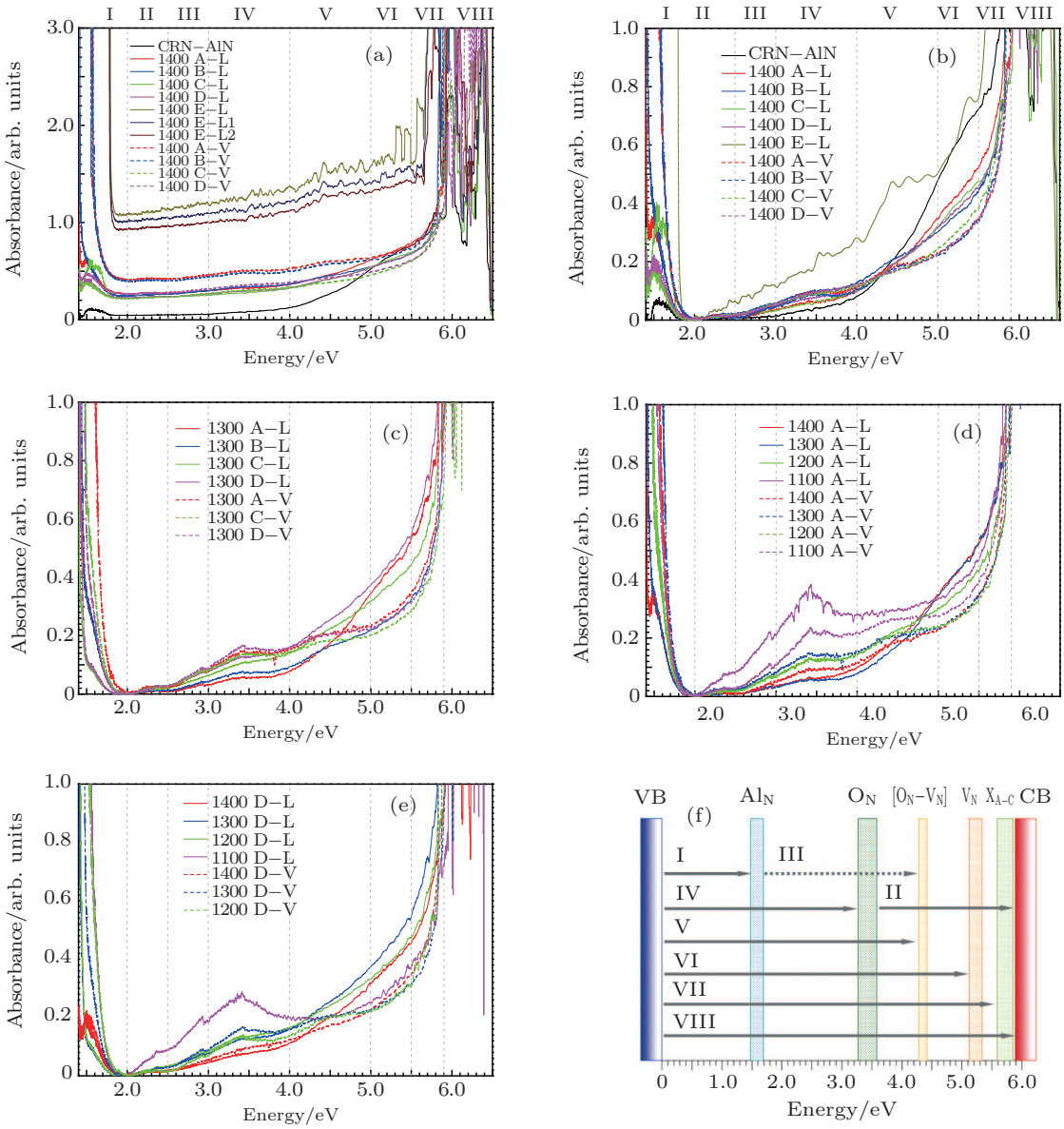


Fig. 4. (color online) Absorption spectra of AlN powders, where (a) the original absorption spectra of AlN produced at 1400 °C reveal that all absorption curves are similar in shape and have minima around 2.0 eV, and that all curves of V samples lie above those of their corresponding L samples in a range between 1.90 eV and 4.20 eV; (b) the absorption spectra indent onto the transversal axis from the spectra in panel (a); the absorption spectra of AlN are produced (c) at 1300 °C, (d) in NH_3 atmosphere, and (e) in mixture atmosphere. All spectra could be divided into eight zones in consideration of their different behaviors and panel (f) shows the defect energy levels within bandgap diagram of AlN and relevant transitions corresponding to the spectra.

(I) Optical absorption

The spectra can be divided into eight zones marked from I to VIII, which have different centers and distinct behaviors with the change of nitridation temperature and atmosphere as shown in Fig. 4. The absorbance in each zone exhibits a broad band that could comprise several peaks, while the behavior of the zone is determined by the dominant peak of the band. Zone VIII exceeding 5.90 eV is the conduction band and zone VII includes near bandgap edge and three free excitons X_A, X_B, and X_C.[37–40]

We assign zone VI centered about 5.30 eV to N vacancy (V_N) related transition for several reasons. First, absorbance in this zone is very high and it should be dominated by major defects related to N, Al or O. Second, all of the spectra in Fig. 4 show that absorbances of CRN-AlN and L samples are higher than those of V samples in zone VI. This characteristic is consistent with the conclusion that N concentration in L sample is lower than that in V sample. Meanwhile, this characteristic contradicts the EDX result that O content value in CRN-AlN is lower than in DN-AlN and the conclusion that O concentration is higher in V sample than in their corresponding L sample. Thirdly, the curves of V samples are concentrative and those of L samples are dispersive. This characteristic is in accordance with the conclusion that N diffusion is easy and fast in the vapor phase, leading to high N concentration in V sample. In contrast, N diffusion in the liquid phase is difficult and N

concentration in L sample is greatly dependent on nitridation temperature. Finally, the concentration of Al related defects in CRN-AlN is believed to be lower than that of N related defects. That means the absorbance could not be attributed to O or Al defects since absorbance of CRN-AlN in this zone is much higher than in other zones except for conductive band. Altogether, only V_N should be responsible for the absorption band in this zone. This assignment accords with that given by Bastek *et al*[41] who studied the CL spectra of AlN epilayers at 5-K temperature and found that V_N band located at about 5.0 eV increases in Al-rich atmosphere. Bickermann *et al*[42] discussed the OA spectra of bulk AlN single crystal and ascribed the 5.2-eV band to V_N- or O-related defects.

The behavior of this V_N-related absorption band provides an insight into the reaction process and OA properties of the products. As figures 4(b) and 4(c) show, the absorption is atmosphere-dependent at different temperatures. For 1400 E–L sample, its highest absorbance indicates the highest V_N concentration, which results from very low N_2 dissociation rate and local N concentration. B-L samples have lower absorbance than other L samples, implying that the presence of NH_3 could produce maximal N concentration in the mixture via the catalysis-aided dissociation of N_2. On the other hand, the absorbance of all V samples in the zone are close to each other and lower than that of L samples, indicating that low V_N concentration is caused by N-rich atmosphere. The results accord well with those from the proposed reaction model in Subsection 3.2 and the agreement further supports our assignment of V_N.

Zone IV situated around 3.40 eV is ascribed to O_N-related transition for several reasons. First, the characteristic that CRN-AlN has the lowest absorbance in the zone (see Fig. 4(b)), which is consistent with the fact that all CRN-AlN samples have the lowest O content values. Second, in all cases except for 1100 °C, the absorbances of V samples are higher than those of their corresponding L samples as shown from Fig. 4(b) to Fig. 4(e). This is consistent with the conclusion that O is rich in atmosphere. Meanwhile, for 1100 A–L, 1100 A–V, and 1100 D–L in Figs. 4(d) and 4(e), the absorbances are much higher than others and the absorbances of 1100 A–L are higher than those of 1100 A–V. This characteristic accords well with the fact that O contamination is hard to reduce and expel from Al liquid by NH_3 when the temperature of 1100 °C is too low to trigger the convective transportation. Thirdly, the absorbances of 1400 A–L and 1300 A–L are lower than those of other L samples as shown in Figs. 4(b) and 4(c). This characteristic is consistent with the fact that H content value in A atmosphere is the highest and convective transportation is triggered beyond 1200 °C, leading to remarkable O elimination in 1400 A–L and 1300 A-L samples. Finally, the absorbances of L and V samples decrease with the increase of nitridation temperature, which is in good agreement with the conclusion in the previous study that O content of AlN decreases with the increase of its nitridation temperature.[32] In summary, the absorbance behavior in this zone is in accordance with those of O content and O_N concentration in the samples. In addition, the absorbance behaviors in zones II and III follow that in zone IV except for smaller absorbance variation, suggesting that they are related to the behavior of O_N.

However, we should note that the assignment of O_N is controversial among many researchers. Shi *et al*[28] conducted PL and CL measurements on AlN nano-tips and claimed that O_N is responsible for the transition around 3.4 eV, and that the transition results from [O_N–V_{Al}] complex to isolated O_N ionic level. Bellucci *et al*[29] ascribed 3.4-eV bands in CL spectrum of commercial AlN powder and nano powders to a complicated donor–acceptor pairs related to O defect. Senawiratne *et al*[43] also denied that the 3.5-eV peak on PL spectrum of bulk AlN single crystal depended solely on O defects.

As for zone V, its absorbance is moderate and relatively stable in comparison with those in zones VI and IV. Further observation found that the band located around 4.40 eV acted as pivot of a seesaw and the absorbance before and after this band behaved like a seesaw. Taking Fig. 4(c) for example, 1300 A–L is lower than 1300 B–L in zone IV before their crossover point at 4.40 eV (called pivot), whereas their location is reversed in zone VI after the pivot. The absorbance in zone V increases or decreases only when absorbances in VI and IV both acted in the same way. Therefore, we predict a new donor named [V_N–O_N] complex for the absorption band around 4.40 eV. The concentration of this complex is controlled by the concentrations of V_N and O_N. They are related by the following equation:

$$\{[V_N - O_N]\} = k \cdot \{V_N\} \cdot \{O_N\}, \tag{7}$$

where k is a proportionality coefficient, $\{V_N\}$, $\{O_N\}$, and $\{[V_N–O_N]\}$ are the concentrations of V_N, O_N, and their complex respectively. In another aspect, the absorbances of VI and IV are in inverse-proportional relation, meaning that a competition mechanism for N site could exist between O_N and V_N in the same sample. When O_N is kicked out from the N site, an N atom was not always ready to fill in the site and thus V_N is produced.

On the other hand, [V_{Al}–O_N] rather than [V_N–O_N] complex was cited commonly,[28,42,44,45] perhaps because V_{Al} was the dominant vacancy and formation of [V_{Al}–O_N] was energy-favorable action in those research studies. This could not be true in our samples. Theoretically, the formation energy of the complex arises from Coulomb interactions, thus [V_N–O_N] complex could come into being if V_N and O_N are in opposite charge states. Calculations show that V_N and O_N could be in positive and negative charge state.[46,47] Therefore, we

tentatively predict that the [V_N–O_N] is responsible for the absorption at 4.40 eV.

Till now, the characteristics corresponding to V_N, O_N, and their complex have been found in the spectra. However, Al-related defects as the major defect and zone I in the spectra need to be identified. Since CRN-AlN has the lowest but apparent absorbance and 1400 E–L shows the highest absorbance near 1.50 eV, we assign the zone to Al_N rather than Al_i from the consideration of the formation of the latter which is energy unfavorable to CRN-AlN. Another proof is that Al_N acted as a deep acceptor in AlN[17] while Al_i acted as a shallow donor.[19,20,23]

Consequently, although we cannot yet definitely determine the energy levels of the defects nor the relationship between the transitions and absorption, we can tentatively develop a possible energy band diagram with the defect levels of our DN-AlN as shown in Fig. 4(f). Therefore, we can tentatively establish the relationship between optical transitions and the zones in OA spectra. The energy band diagram is arranged horizontally with a hypothetical energy axis for the convenience of its comparison with the OA spectra. Since OA spectra are collected from 1.40 eV to 6.50 eV, those transitions out of the range are not shown in the diagram. Each dominant band of the zones in OA spectra finds its corresponding transition well except in zone III which is located around 3.0 eV. It was tentatively ascribed to the transition of donor–acceptor pair of [Al_N] and [O_N–V_N], which is consistent with the result of AlN nanowire.[31]

(II) PL analysis

In order to further realize and identify the defect-related optical properties of the products, PL measurement is conducted at room temperature and the spectrum is collected in an energy range from 1.90 eV to 3.80 eV. The PL spectra in Figs. 5(a) and 5(b) could be divided into three zones labeled from i to iii, whose characteristics are similar to counterparts of their OA spectra in the same energy range as that shown in Fig. 5(c). If we deduct the absorbance background of the curves in Fig. 5(c), it is revealed that the behaviors of PL spectra accord well with counterparts of their OA spectra in the respect of band location and intensity. Therefore, we can explain the PL spectra with the defect-related transitions in the band diagram as shown in Fig. 5(d).

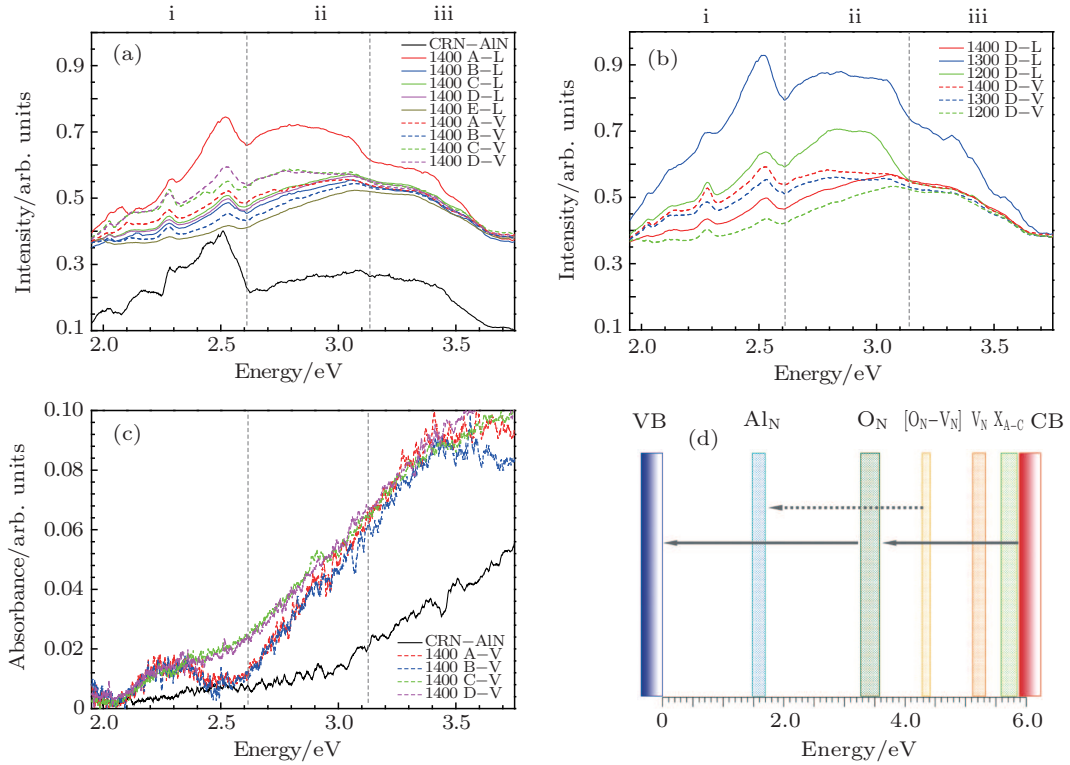


Fig. 5. (color online) Photoluminescence spectra of AlN powders produced (a) at 1400 °C, (b) in mixed atmosphere, (c) optical absorption spectra of AlN in the same energy range, panel (d) shows the defect levels and related transitions corresponding to the PL spectra.

However, we should note that the PL spectrum has fine structure and complicated behavior, which cannot be simply corresponding to those of their OA counterparts. To further understand and identify the defect-related optical properties, it is necessary to perform a detailed study in full range spectrum of CL or PL with excitation wavelength shorter than 200 nm.

4. Conclusions

AlN powders are prepared by direct nitridation in mixed atmospheres of N_2 and NH_3 with different NH_3/N_2 ratios. Full nitridation is accomplished beyond 1200 °C and two kinds of AlN powders are produced in the crucible and at the brim of the crucible through liquid and vapor phase reactions respec-

tively. NH_3 acts as a catalyst for N_2 dissociation and a maximum of reactive N content value could be obtained in the mixture. Meanwhile, NH_3 is conducible to the elimination of O contamination via reduction process. A comprehensive reaction model of direct nitridation is proposed. The products are Al-rich and composition-tunable nonstoichiometric AlN in which N, O, and Al content values and their relevant defect concentrations change with nitridation atmosphere and temperature. Therefore, distinct features and behaviors related to the defects are found in the optical spectra. Through the comparison of optical spectra of the AlN powders, it is proposed that V_N and O_N donors are respectively located around 5.30 eV and 3.40 eV and Al_N acceptors are located about 1.50 eV. A new donor complex named [V_N–O_N] is predicted to be at 4.40 eV within the 5.90-eV bandgap at room temperature. It is also demonstrated that comparison analysis of optical spectra of nonstoichiometric AlN rather than the nominal stoichiometric one should be efficient at the identification of defects' energy levels.

References

[1] Ruterana P 2003 *Nitride Semiconductors Handbook on Materials and Devices* (Weinheim: John Wiley & Sons) pp. 171–174

[2] Nakamura S 2000 *Introduction to Nitride Semiconductor Blue Lasers and Light Emitting Diodes* (New York: CRC Press) pp. 12–15

[3] Liu B, Zhang S, Yin J Y, Zhang X W, Dun S B, Feng Z H and Cai S J 2013 *Chin. Phys. B* **22** 057105

[4] Taniyasu Y, Kasu M and Makimoto T 2006 *Nature* **441** 325

[5] Ren F, Hao Z B, Hu J N, Zhang C and Luo Y 2010 *Chin. Phys. B* **19** 116801

[6] Taniyasu Y and Kasu M 2011 *Appl. Phys. Lett.* **98** 131911

[7] Georgieva A K, Ciechonski R R and Fosberg U 2009 *Cryst. Growth Des.* **9** 880

[8] Wu B, Noveski V, Zhang H, Schlesser R, Mahajan S, Beaudoin S and Sitar Z 2005 *Cryst. Growth Des.* **5** 1491

[9] Shatskiy A, Borzdov Y M, Yamazaki D, Litasov K D, Katsura T and Palyanov Yuri N 2010 *Cryst. Growth Des.* **10** 2563

[10] Bickermann M, Epelbaum B M, Filip O, Heimann P, Nagata S and Winnacker A 2010 *Phys. Status Solidi C* **7** 1743

[11] Hartmann C, Wollweber J, Seiz C, Albrecht M and Fornari R 2008 *J. Cryst. Growth* **310** 930

[12] Sōmiya S, Aldinger F, Claussen N, Spriggs R M, Uchino K, Koumoto K and Kaneno M 2003 *Handbook of Advanced Ceramics,* Volume II*: Processing and Their Applications* (Kidlington: Elsevier Academic Press) pp. 3–9

[13] Iriarte G F, Rodríguez J G and Calle F 2010 *Mater. Res. Bull.* **45** 1039

[14] Pietranico S, Pommier S, Lefebvre S, Khatir Z and Bontemps S 2009 *Int. J. Fatigue* **31** 1911

[15] Eriguchi K, Hiratsuka T, Murakami H, Kumagai Y and Koukitu A 2008 *J. Cryst. Growth* **310** 4016

[16] Siwiec J, Sokolowska A, Olszyna A, Dwilinski R, Kaminska M and Konwerska-Hrabowska J 1998 *Nanostruct. Mater.* **10** 625

[17] Yao Z Q, Li Y Q, Tang J X, Zhang W J and Lee S T 2008 *Diam. Relat. Mater.* **17** 1785

[18] Sun J, Wu J, Ling H, Shi W, Ying Z F and Li F M 2001 *Phys. Lett. A* **280** 381

[19] Senawiratne J 2006 "Structural and Optical Characterization of Group III-Nitride Compound Semiconductors" (Ph. D. dissertation) (Atlanta: Georgia State University)

[20] Strassburg M, Senawiratna J, Dietz N, Haboeck U, Hoffmann A, Noveski V, Dalmau R, Schlesser R and Sitar Z 2004 *J. Appl. Phys.* **96** 5870

[21] Bichmann M, Münch A, Epelbaum B M, Filip O, Heimann P, Nagata S and Winnacker A 2008 *J. Appl. Phys.* **103** 0735221

[22] Sitar Z, Moody B, Craft S, Schlesser R, Dalmau R, Xie J, Mita S, Rice T, Tweedy J, LeBeau J, Hussey L, Collazo R, Gaddy B and Irving D 2012 4th *International Symposium on Growth of III-Nitrides*, July 16–19, 2012, St. Petersburg, Russian, p. 16

[23] Nappé J C, Grosseau Ph, Benabdesselam M, Beauvy M and Guilhot B 2009 *Proceedings of the* 11th *ECERS Conference*, Krakow, p. 1105

[24] Honma T, Kuroki Y, Okamoto T, Takata M, Kanechika Y, Azuma M and Taniguchi H 2008 *Ceram. Int.* **34** 943

[25] Sikalidis C 2011 *Advances in Ceramics-Characterization, Raw Materials, Processing, Properties, Degradation and Healing* (Rijeka: InTech) pp. 59–66

[26] Lü H M, Chen G D, Yan G J and Ye H G 2007 *Chin. Phys.* **16** 2814

[27] Li X F, Kong L N, Shen L H, Yang J H, Gao M, Hu T J, Wu X T and Li M 2013 *Mater. Res. Bull.* **48** 3310

[28] Shi S C, Chen C F, Chattoadhyay S, Chen K H, Trinkler L and Berzina B 2006 *Appl. Phys. Lett.* **89** 1631271

[29] Bellucci S, Popov A I, Balasubramanian C, Cinque G, Marcelli A, Karbovnyk I, Savchyn V and Krutyak N 2007 *Radiat. Meas.* **42** 708

[30] Qiao Z J, Chen G D, Ye H G, Wu Y L, Niu H B and Zhu Y Z 2012 *Chin. Phys. B* **21** 087101

[31] Kim H W, Kebede M A and Kim H S 2009 *Appl. Surf. Sci.* 7221

[32] Zhang D, Liu F M, Cai L G, Liu X Q and Li Y 2013 *J. Alloys Compd.* **547** 91

[33] Kimura I, Ichiya K, Ishii M and Hotta N 1989 *J. Mater. Sci. Lett.* **8** 303

[34] Chang A J, Rhee S W and Baik S 1995 *J. Mater. Sci.* **30** 1180

[35] Hiroki H, Yasushi K, Keiichi E and Yonenaga I 2007 *J. Appl. Phys.* **102** 0261031

[36] Chen L 2005 "Optical Characterization of Gallium Nitride, Silicon Carbide and Aluminum Nitride" (Ph. D. dissertation) (Tempe: Arizona State University)

[37] Chen L, Skromme B J, Dalmau R F, Schlesser R, Sitar Z, Chen C, Yang J, Sun W, Khan M A, Nakarmi M L, Lin J Y and Jiang H X 2004 *Appl. Phys. Lett.* **85** 4334

[38] Silveira E, Freitas J A Jr and Glembocki O J 2005 *Phys. Rev. B* **71** 0412011

[39] Prinz G i M, Ladenburger A, Feneberg M, Thonke K, Sauer R, Taniyasu Y, Kasu M and Makimoto T 2006 *Superlattices Microstruct.* **40** 513

[40] Tang X, Hossain F, Wongchotigul K and Spencer M G 1998 *Appl. Phys. Lett.* **72** 1501

[41] Bastek B, Bertram F, Christen J, Hempel T, Dadgar A and Krost A 2009 *Appl. Phys. Lett.* **95** 0321061

[42] Bickermannl M, Epelbaum B M, Filip O, Heimann P, Nagata S and Winnacker A 2009 *Phys. Status Solidi B* **246** 1181

[43] Senawiratne J, Strassburg M, Dietz N, Haboeck U, Hoffmann A, Noveski V, Dalmau R, Schlesser R and Sitar Z 2005 *Phys. Status Solidi C* **2** 2774

[44] Uedono A, Ishibashi S, Keller S, Moe C, Cantu P, Katona T M, Kamber D S, Wu Y, Letts E, Newman S A, Nakamura S, Speck J S, Mishra U K, DenBaars S P, Onuma T and Chichibu S F 2009 *J. Appl. Phys.* **105** 0545011

[45] Mäki J. M, Makkonen I, Tuomisto F, Karjalainen A, Suihkonen S, Räisänen J, Chemekova T Y and Makarov Y N 2011 *Phys. Rev. B* **84** 0812041

[46] Mattila T and Nieminen R M 1996 *Phys. Rev. B* **54** 16676

[47] Stampfl C and van de Walle C G 2002 *Phys. Rev. B* **65** 1552121